High glucose induces adipogenic differentiation of muscle-derived stem cells

Paola Aguiari*, Sara Leo*, Barbara Zavan†, Vincenzo Vindigni‡, Alessandro Rimessi*, Katiuscia Bianchi*, Chiara Franzin§, Roberta Cortivo†, Marco Rossato§, Roberto Vettor§, Giovanni Abatangelo†, Tullio Pozzan¶‖, Paolo Pinton*, and Rosario Rizzuto*‖

*Department of Experimental and Diagnostic Medicine, Interdisciplinary Center for the Study of Inflammation, University of Ferrara, 44100 Ferrara, Italy; †Department of Histology, Microbiology and Medical Biotechnologies, University of Padua, 35122 Padua, Italy; ‡Clinic of Plastic Surgery, University of Padua, 35122 Padua, Italy; §Endocrine-Metabolic Laboratory, Internal Medicine, Department of Medical and Surgical Sciences, University of Padua, 35122 Padua, Italy; and ¶Department of Biomedical Sciences, CNR Institute of Neuroscience, and Venetian Institute of Molecular Medicine, University of Padua, 35122 Padua, Italy

Contributed by Tullio Pozzan, December 5, 2007 (sent for review September 14, 2007)

Regeneration of mesenchymal tissues depends on a resident stem cell population, that in most cases remains elusive in terms of cellular identity and differentiation signals. We here show that primary cell cultures derived from adipose tissue or skeletal muscle differentiate into adipocytes when cultured in high glucose. High glucose induces ROS production and PKCβ activation. These two events appear crucial steps in this differentiation process that can be directly induced by oxidizing agents and inhibited by PKCβ siRNA silencing. The differentiated adipocytes, when implanted *in vivo*, form viable and vascularized adipose tissue. Overall, the data highlight a previously uncharacterized differentiation route triggered by high glucose that drives not only resident stem cells of the adipose tissue but also uncommitted precursors present in muscle cells to form adipose depots. This process may represent a feed-forward cycle between the regional increase in adiposity and insulin resistance that plays a key role in the pathogenesis of diabetes mellitus.

adipocyte | hyperglycemia | PKC | ROS

The identity and regulation of the adipocyte precursor cell is a topic of great interest and intense study. Microarray analyses and functional genomics have revealed adipogenic transcriptional signatures (1), but the signals occurring in pathophysiological conditions and aging are still incompletely understood. Stem cells are present in the adipose tissue and, under appropriate differentiation, signals can differentiate *in vitro* in adipocytes or other mesenchimal cells. Adipose-derived stem cells (ADSCs) represent the key cellular element for the control of body adiposity and they may substitute bone marrow-derived stem cells in their promising applications for tissue repair and regeneration. Indeed, s.c. adipose depots are accessible and abundant, thereby providing a potential adult stem cell reservoir for each individual.

Further complexity is added by the observation that the adipose depots of the body differ in functional properties, reflecting the existence of different subpopulations of adipocytes. Visceral and s.c. adipocytes release different endocrine mediators, collectively called adipokines. Although both adipose depots are correlated with metabolic risk factors, visceral adipose tissue remains more strongly associated with an adverse metabolic risk profile, type 2 diabetes development, and an increased risk of coronary heart disease (2). Even more intriguing is the role of intramyocellular triglycerides and intramuscular fat, given that intramuscular fat stores and substitution of muscle with adipose tissue have been reported to strongly correlate with insulin resistance (3). Thus, in the context of diabetogenesis (but also for other metabolic or myodystrophic conditions), key biological issues are how intra- and intermuscular adipose tissues originate and proliferate. Attention has been recently focused on the transdifferentiation of muscle progenitors to the adipogenic lineage, given that myopathic skeletal muscle is characterized by the replacement of myofibers by adipose tissue (4).

Muscle-derived stem cells (MDSCs) include the so-called satellite cells, i.e., the precursor cells capable of differentiating *in vivo* to mature muscle fibers and *in vitro* up to multinucleated skeletal myotubes (5). Human satellite cells retain broad differentiation capacity, including the generation of adipocytes in appropriate culture conditions (adipogenic medium) in a process that is enhanced by the insulin sensitizer rosiglitazone (6). Activators of PPAR-γ cause, in muscle, the induction of genes involved in fatty acid uptake, storage, and metabolism (7), and the myogenic cell line C2C12 can be converted to adipocytes by overexpression of PPAR-γ and C/EBP (8). As in hyperglycemia, high-glucose concentrations up-regulating sterol regulatory element binding protein 1c (SREBP-1c) induce *de novo* lipogenesis and intracellular lipid accumulation in contracting myotubes (9).

We here demonstrate that both ADSCs and MDSCs differentiate into adipocytes upon high glucose exposure. In this process, an important role is attributed to reactive oxygen species (ROS) and downstream effector kinases, such as PKCβ, recently shown to act as signaling link between ROS and mitochondrial targets implicated in age-dependent organ deterioration (10).

Results

High Glucose Induces Adipocyte Differentiation of Stem Cells from Adipose Tissue. The isolation of ADSCs from human lipoaspirates and their *in vitro* differentiation capacity into various mesenchimal tissues was first established by using standard protocols. To maximize nutrients delivery and to mimic the dynamic stress conditions stimulating formation of extracellular matrix, ADSCs were seeded onto hyaluronan-based sponge in a perfusion system that allows the circulation of culture medium through the scaffold (bioreactor). Further details on the isolation procedure and bioreactor are given in *Materials and Methods*. Under these conditions, the classical adipogenic, osteogenic, and chondrogenic media were highly efficient in causing specific differentiation into the expected cell lineage, as confirmed by morphological criteria (histological and electron microscopy analyses) and molecular hallmarks. Similar data have been obtained by us and others, using ADSC from mouse or rats, or using more standard culture conditions (11). The procedures used and the full characterization of the differentiated mesenchimal cells are described in supporting information (SI) Fig. 6.

Author contributions: P.A., S.L., and B.Z. contributed equally to this work; P.P. and R.R. designed research; P.A., S.L., B.Z., V.V., A.R., K.B., and C.F. performed research; P.A., S.L., B.Z., A.R., R.C., M.R., R.V., G.A., T.P., and P.P. analyzed data; and R.R. wrote the paper.

The authors declare no conflict of interest.

‖To whom correspondence may be addressed. E-mail: tullio.pozzan@unipd.it or rzr@unife.it.

This article contains supporting information online at www.pnas.org/cgi/content/full/0711402105/DC1.

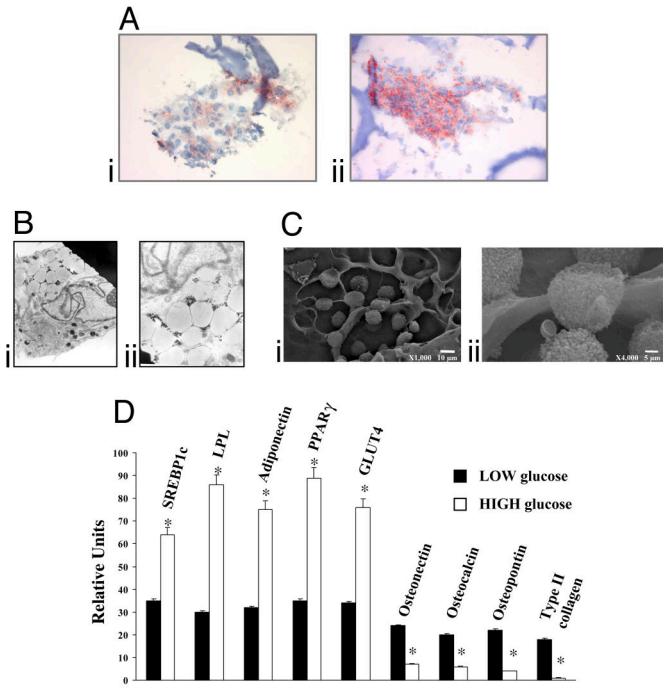

Fig. 1. Adipose-derived Stem Cells (ADSCs) cultured on Hyaff 11 sponges in LG- and HG-DMEM. (*A*) Oil red O staining of ADSCs grown in LG-DMEM (*i*) or HG-DMEM (*ii*). Lipid droplets are in red, and biomaterial fibers in blue. (Magnification: ×20.) (*B*) Transmission electron microscopy (TEM) of two representative fields. (Magnification: ×6,500.) (*C*) Scanning Electron microscopy (SEM) of ADSCs at two different magnifications. (*D*) mRNA expression of adipogenic, chondrogenic, and osteogenic markers analyzed after 14 days by semiquantitative real time PCR in ADSCs cultured on 3D scaffolds in LG- and HG-DMEM. Results for each condition are from quadruplicate experiments, and values are expressed in relative units as the mean ± SD. *, $P < 0.05$.

The physiological stimuli that control ADSCs differentiation into adipocytes *in vivo* remain unknown. We investigated whether one of the most common conditions leading to an increase in adipose tissue (12) *in vivo*, i.e., high-glucose concentration, can affect human ADSCs differentiation into mature adipocytes *in vitro* (Fig. 1). ADSCs were maintained for 14 days in a low-glucose (LG)-DMEM (i.e., DMEM, 10% FBS, and 5.5 mM glucose) or in a high-glucose (HG)-DMEM (i.e., DMEM, 10% FBS, and 25 mM glucose), and then analyzed by morphological (histochemistry, Fig. 1*A*, and electron microscopy, Fig. 1 *B* and *C*) and molecular (Fig. 1*D*) approaches. Staining with oil red O (ORO), selective for triglyceride depots, revealed substantial adipose differentiation in cells grown in HG-DMEM (Fig. 1*Aii*, 4.18 ± 0.21 OD at 520 nm), compared with cells grown in lower glucose DMEM (LG-DMEM) (Fig. 1*Ai*, 2.16 ± 0.11 OD at 520 nm). Accordingly, EM analysis showed numerous cells with a typical adipocytic phenotype, i.e., containing large lipid droplets surrounded by a thin ring of cytoplasm (Fig. 1*B*). SEM microscopy showed a population of rounded cells of various sizes, i.e., the typical appearance of adipose tissue (Fig. 1*C*). The lower magnification (Fig. 1*Ci*) reveals the presence of round adipocytes on both sides of the specimen.

In high-glucose conditions, RT-PCR analysis of mRNA transcripts (Fig. 1*D*) revealed significant expression of adipocyte-specific proteins, such as peroxisome proliferators activated receptor gamma (PPARγ), lipoprotein lipase (LPL), adiponectin, glucose transporter 4 (GLUT4), and SREBP1c. Conversely, chondrogenic (type II collagen) and osteogenic markers (osteopontin, osteonectin, and osteocalcin) were down-regulated in HG-DMEM compared with cells cultured in LG-DMEM.

Adipogenic Conversion of Muscle-Derived Stem Cells on High Glucose. We concluded that incubation in high glucose *per se* can drive the differentiation of uncommitted stem cells into adipocytes, a previously uncharacterized mechanism for ADSCs (but see refs. 13 and 14 for pancreatic β cell lines). However, these stem cells were derived from adipose tissue, and thus the observed effect could represent the enhancement of the default differentiation route of adipocyte precursors. To investigate whether it reflected conversely the differentiation of uncommitted mesenchimal precursors or even the transdifferentiation of stem cells of other mesenchimal tissues, we turned our analysis to primary cultures of skeletal muscle. These cells can be easily obtained from animal models, and thus the following experiments were carried out on cells derived from neonatal rats. Muscle-derived stem cells (MDSCs) from mouse or rats can be differentiated into large myotubes, carrying most phenotypic properties of skeletal muscle in terms of contractile protein expression, morphological aspect (with diad and triad formation), and signaling properties (5).

In the experiments shown in Fig. 2, we analyzed the effect of HG-DMEM on MDSCs, using the standard culture conditions, i.e., in 100-mm Petri dishes. Parallel batches of cells were maintained in LG-DMEM. In both cases, the medium was supplemented with 10% FCS (a conditions that prevents differentiation into myotubes), and cells were maintained in culture for 18–25 days before analysis. In LG-DMEM, as revealed by either counting the cells with large vacuoles in the cytoplasm (Fig. 2*Ai*) or those positive for the lipid specific dye 4,4-difluoro-1,3,5,7,8-pentamethyl-4-bora-3a,4a-diaza-*s*-indacene (BODIPY) (Fig. 2*Aii*) the percentage of cells with a morphological adipocyte phenotype was only 3.3 ± 2.4%. In HG-DMEM, a highly significant increase in adipocyte differentiation was detected: 9.2 ± 2.9% of the cells showed a clear adipocytic phenotype, with either analysis methods (Fig. 2*B*), 2- to 4-fold higher than in LG-DMEM (HG: $n = 6$; LG: $n = 4$).

We then verified adipose differentiation efficiency in the 3D scaffold of the bioreactor. MDSCs were thus seeded onto the hyaluronan-based sponge and maintained in culture for 14 days under LG-DMEM or HG-DMEM perfusion. Then, histochemical and ultrastructural analyses of the cell culture were carried out. For the former, five randomly chosen fields were analyzed for each conditions, and the experiment was repeated with identical results in three different trials. The results of a typical experiment are presented in Fig. 2. In LG-DMEM, oil red O staining was hardly detectable (Fig. 2*Ci*) although the cells became loaded with lipid vesicles in HG-DMEM, as revealed by oil red O staining (Fig. 2*Di*); quantification of oil red O-stained cells showed a marked higher percentage of adipocytes in HG-DMEM (3.87 ± 0.31 OD at 520 nm) compared with LG-DMEM (1.89 ± 0.15 OD at 520 nm). In agreement with these observations, electron micrographs showed mostly elongated fibroblast-like cells in LG-DMEM (Fig. 2*Cii*) and a high fraction of rounded cells with the typical mature adipocytes appearance, in HG-DMEM (Fig. 2*Dii*). The percentage of cells with an adipocyte phenotype obtained with HG-DMEM from muscle cultures did not differ significantly from that observed under the same conditions, using ADSCs (3.87 ± 0.31 OD at 520 nm in MDSCs and 4.18 ± 0.21 OD at 520 nm for ADSCs), indicating that the differentiated adipocytes in the former case cannot derive from a contamination from adipose tissue in the muscle cell cultures.

The adipogenic potential of high glucose on MDSCs was confirmed also by RT-PCR analyses of adipocyte-specific transcripts: cells cultured in the bioreactor and maintained in HG-DMEM (Fig. 2*E*) for 7 and 14 days, shown an higher expression of PPARγ, LPL, adiponectin, GLUT4, and SREBP1c and a down-regulation of chondrogenic and osteogenic markers, compared with cells grown in LG-DMEM. Expression of the adipocyte markers is shown in Fig. 2*E* for 14 days of analysis. The comparison of the RT-PCR data at 7 and 14 days both for the ADSCs (Fig. 1) and the MDSCs (Fig. 2) is presented in SI Fig. 7.

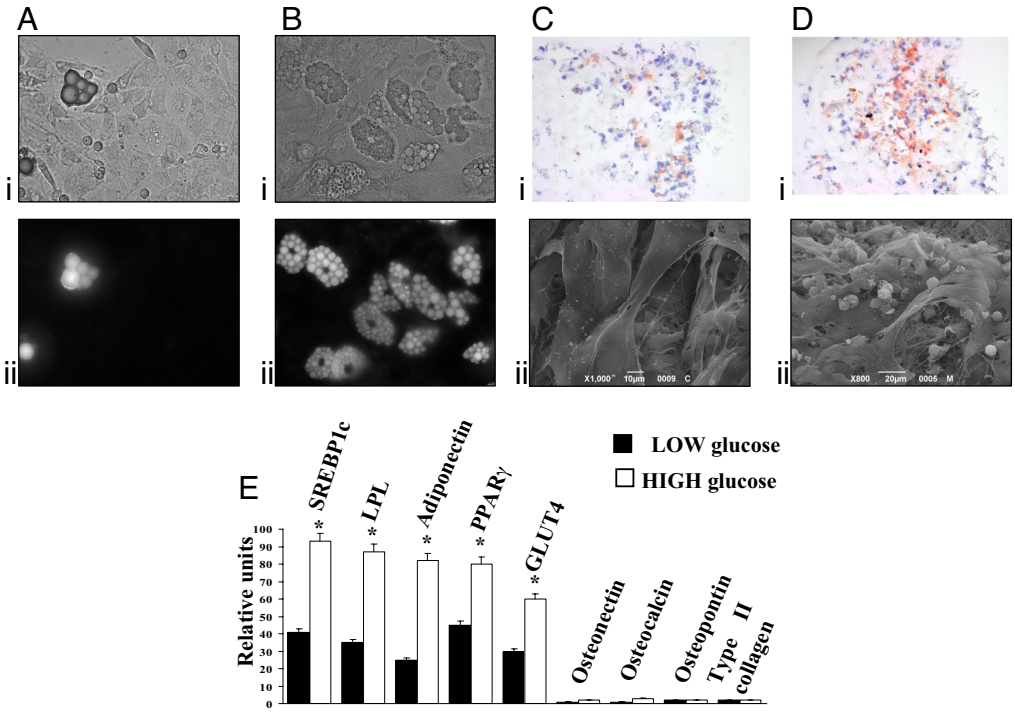

Fig. 2. High glucose induces adipocyte differentiation of muscle-derived stem cells (MDSCs). (*A* and *B*) Phase-contrast image (*i*) and BODIPY staining (*ii*) of MDSCs cultured in LG-DMEM (*A*) or HG-DMEM (*B*). (*C* and *D*) Oil red O staining (*i*) and SEM analysis (*ii*) of MDSCs cultured for 14 days on Hyaff 11 sponges in LG-DMEM (*C*) and HG-DMEM (*D*). Lipid droplets are in red, and nuclei are in blue. (Magnification: ×40). (*E*) Adipogenic, chondrogenic, and osteogenic markers mRNA expression analyzed by semiquantitative real time PCR in MDSCs cultured on 3D scaffolds for 14 days in LG- and HG-DMEM. Results for each condition are from quadruplicate experiments, and values are expressed in relative units as the mean ± SD. *, $P < 0.05$.

Oxidative Stress by Effector PKCs Is a Trigger of Adipocytic Differentiation. We decided to use this cell model to get some insight into the mechanisms that drive high-glucose-induced adipocytic differentiation. In the past years, major attention has been dedicated to the induction of oxidative stress by high glucose (through three mechanisms, NADP(H)oxidase, xanthine oxidase, and the mitochondrial respiratory chain) and its relevance for the development of diabetes complications. Regarding the effector mechanisms, PKC isoforms (PKCβ and PKCδ in particular) have been shown to be activated by oxidizing conditions (10). We thus verified whether these mechanisms represent the signaling route in stem cells differentiation to adipocytes. We first measured ROS production during high-glucose incubation. MDSC were obtained as in Fig. 2, but the cells were seeded onto 24-mm glass coverslip for microscopic analysis. Seven days after seeding, cells cultured in LG-DMEM or HG-DMEM were loaded with the ROS-sensitive fluorescent probe CM-H_2DCFDA. The coverslip with the cells was transferred to the stage of a confocal microscope, and fluorescence emission at 520 nm was monitored, revealing continuous ROS production. The results, shown in Fig. 3*A*, demonstrated that ROS production is markedly higher if the cell culture is maintained in HG-DMEM.

We then verified whether this condition activates PKCβ, as observed in endothelial cells (15). Endogenous PKCβ revealed by immunofluorescence was mostly cytosolic in MDSCs maintained in LG-DMEM (Fig. 3*Bi*). Incubation for 1 h in 25 mM glucose induced a partial translocation of the kinase to the plasma membrane in ≈30% of the cells (Fig. 3*Bii*), with a pattern similar to that observed upon direct activation by phorbol 12-myristate 13-acetate (PMA) (Fig. 3*Biii*).

The simplest interpretation of the data are that ROS produced in response to high glucose, by stimulating PKCβ (and possibly other effectors), act as a differentiation signal for adipogenic conversion of MDSCs. We tested this hypothesis with three approaches: (*i*) LG-DMEM was supplemented with H_2O_2 to test whether it could mimic the effect of high glucose and thus trigger adipocytic differentiation; (*ii*) the cells, maintained in HG-DMEM, were transduced with a vector carrying the PKCβ siRNA to test whether this could inhibit adipocytic differentiation; and (*iii*) the cells in HG-DMEM were transduced with PKCβ expression vector to verify whether its overexpression could synergize with high glucose. The results presented in Fig. 4*A* (quantitated by counting the percentage of BODIPY-loaded cells) strongly support the hypothesis. In particular, (*i*) in LG-DMEM, addition of 100 μM H_2O_2 enhanced the differentiation rate to a level comparable to that observed in high glucose (9.34 ± 2.9% vs. 9.19 ± 2.9%, respectively) and no significant enhancement was detected if H_2O_2 was added to HG-DMEM (10.18 ± 0.5%); (*ii*) PKCβ siRNA, added to cells incubated in HG-DMEM, drastically reduced adipocytic differentiation (−80%) (Fig. 4*A*) to levels below those found in LG-DMEM, whereas an unrelated siRNA (*FHIT*) had no effect (5.5 ± 0.5%); (*iii*) a major (300%) enhancement of lipid-loaded cells was observed in cells overexpressing PKCβ and incubated in HG-DMEM. Infection with a control viral vector (an adenoviral vector expressing mtGFP) and PKCβ, *per se*, did not increase adipocytic differentiation if added to cells in LG-DMEM (data not shown). The same results were obtained by seeding MDSCs onto hyaluronan base sponge of the bioreactor (Fig. 4*B*).

High-Glucose-Differentiated Adipocytes Can Be Successfully Implanted *in Vivo*. Finally, we verified whether *in vitro*-differentiated adipocytes can generate mature and viable adipose tissue *in vivo*. For this purpose, sponges enriched with ADSCs cultured in the bioreactor for 7 days in high glucose, were implanted in the abdominal area of eight female nude rats, as described in *Materials and Methods*. At 1, 2, 3, and 4 weeks after insertion of the graft, the rats were killed and the grafts analyzed macroscopically (for color, ingrowth and vessel formation, weight, and thickness) and micro-

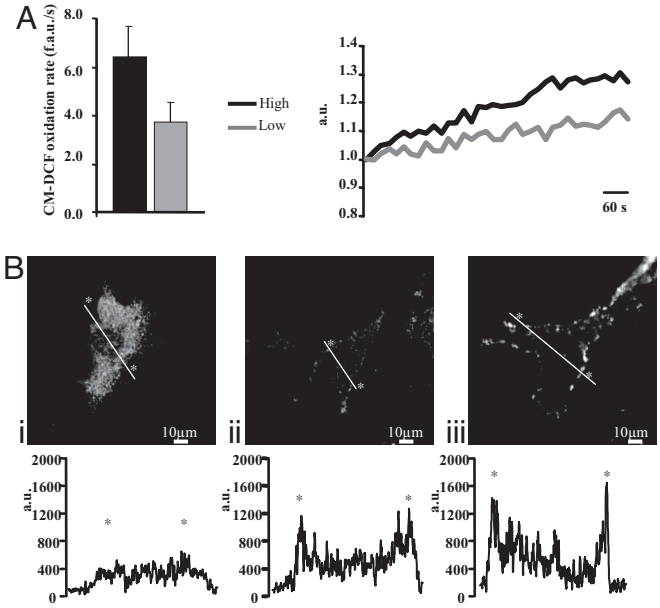

Fig. 3. ROS production of MDSCs cultured in LG- and HG-DMEM and glucose-induced PKCβ-activation. (*A*) Seven days after seeding, cells were loaded with the CM-H_2DCFDA and analyzed by confocal microscopy. Basal ROS production is expressed as mean of CM-DCF oxidation rate (fluorescent arbitrary units per second). Representative traces of CM-DCF oxidation kinetics are shown at *Right* (black, high-glucose condition; gray, low-glucose condition). (*B*) PKCβ membrane translocation, as revealed by immunofluorescence microscopy. Representative images show cells maintained in LG-DMEM (*i*), incubated for 1 h in HG-DMEM (*ii*), and treated with 500 nM PMA (*iii*). The graphs show the quantitation of PKCβ fluorescence intensity along a line crossing the cell (thick white line in the micrograph).

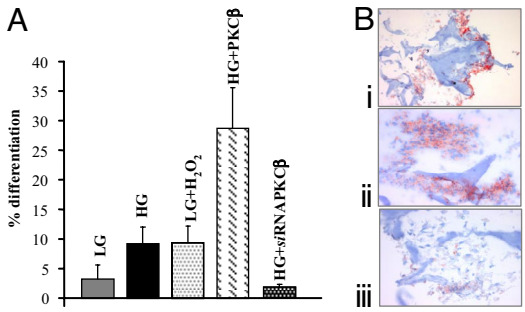

Fig. 4. Quantitation of MDSCs adipocyte differentiation in different conditions. (*A*) MDSCs cultured in different conditions: HG-DMEM, LG-DMEM, LG-DMEM supplemented with 100 μM H_2O_2, PKCβ-overexpression in HG-DMEM, and PKCβ siRNA in HG-DMEM. The efficiency of MDSCs differentiation was quantitated by counting the percentage of BODIPY-loaded cell. The histogram shows the percentage of differentiation $\pm$ SEM. (*B*) MDSCs cultured on Hyaff 11 sponges in LG-DMEM supplemented with 100 μM H_2O_2 (*i*), PKCβ-overexpression in HG-DMEM (*ii*), and PKCβ siRNA in HG-DMEM. Adipogenic differentiation was confirmed by oil red O staining. Lipid droplets are in red, and nuclei are in blue. (Magnification: $\times$10.)

scopically (for pore size, specific and unspecific cellularity, and vascularity). The implant appeared well integrated in the s.c. tissue and not surrounded by fibrotic tissue (Fig. 5*Ai* at 2 weeks and Fig. 5*B* at 3 weeks, white arrows). In addition, numerous capillaries (Fig. 5 *Ai* and *Bi*, blue arrows) revealed significant vascularization of the engineered, reimplanted tissue. Harvesting of the sample confirmed that the sponge maintains its volume and soft consistence and is easily dissected from the surrounding tissue (Fig. 5*Aii*).

Morphological characterization of the explants confirmed a major distribution of preadipocytes over the whole cross-section (Fig. 5*C*). Significant adipose tissue formation was detected (black arrows) (Fig. 5*C*) already at 3 weeks. In most cases, the cells exhibited the hallmarks of mature adipocytes, i.e., a large lipid droplet surrounded by a thin ring of cytoplasm, with a flattened nucleus located at the cell periphery. Adipocytes (Fig. 5*C*, black arrows) were closely attached to the scaffold (red arrows), and multiple capillaries were located near the preadipocytes and adipocytes [Fig. 5 *Ci* and *D* (green arrows)].

Discussion

In this article, we investigated the effect of an increase in glucose concentration on the differentiation route of stem cells residing in both adipose tissue and skeletal muscle. In both cases, a clear induction of adipogenic transformation was observed upon the application of high-glucose culture conditions. The capacity of high glucose to partly activate an adipogenic differentiation program had already been noticed in pancreatic β cells (13, 14). In our case, the process consists in a full conversion into adipocytes, as verified by morphological and molecular criteria and the capacity of these cultured cell to form viable and vascularized adipose depots when implanted *in vivo*. In muscle-derived cells, the process appears to be the genuine differentiation of uncommitted mesenchimal precursors or a transdifferentiation of myogenic precursors. This conclusion is supported by the following evidences: (*i*) when separate cultures were prepared from upper- and lower-limb muscles (the former may be partly contaminated by adipose tissue, whereas the latter is virtually devoid of it), the efficiency of high-glucose-induced adipocytic differentiation was very similar (upper limbs: 8.9 $\pm$ 2.7%; lower limbs 10.3 $\pm$ 1.8%) and (*ii*) the percentage of differentiated adipocytes induced by HG-DMEM is approximately the same whether the culture was derived from muscle or from adipose tissue.

Adult skeletal muscle has a remarkable regenerative capacity, largely mediated by satellite cells residing between the sarcolemma and basal lamina of myofibers (16). The regenerative process and proliferative capacity decrease as a function of age (17), partly for the reduced activity of stimulatory factors (18), with consequent loss of muscle mass. However, these alterations do not account for other features of aged muscle, and, in particular, for the increased lipid content (19). It has been reported that aged mice myoblasts, compared with those from adult mice, show increased expression of genes normally restricted to the adipocyte lineage (20), although a fully differentiated adipocyte phenotype is not achieved. The identification of a primary role of high-glucose exposure in adipocytic differentiation has at least two major important conceptual implications. It shows that high glucose *per se* has an adipogenic potential, thus opening the search for signal transduction pathways operating in obesity and diabetes. Second, a direct link between hyperglycemia and the increase in adiposity highlights a feed-forward cycle, which may play a key role in the progression of the metabolic dysfunction into an irreversible diabetic state.

Regarding the signals driving the differentiation of muscle stem cells into adipocytes, our data suggest a crucial role for reactive oxygen species (ROS). Interestingly, among the cellular consequences of high glucose, increased production of ROS is recognized as a major cause of the clinical complications associated with diabetes and obesity (21). Various mechanisms appear to synergize in increasing ROS production, ranging from the activity of mitochondrial respiratory complexes to the activation of enzymatic systems, such as NOX isoforms, NO synthase, and xanthine oxidase (22). Despite the presence of scavenging systems (e.g., superoxide dismutase and catalase), the damaging effects of ROS have been proposed to be responsible for progressive organ degeneration (23). However, the role of ROS is not only restricted to cell damage induction. Indeed, ROS may directly regulate the activity of transcription factors, such as NF-κB, in turn controlling proinflamma-

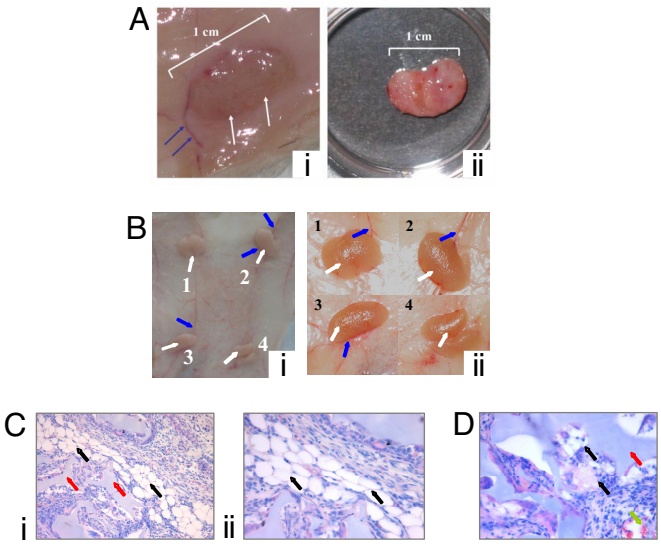

Fig. 5. Macro and microscopic analyses of *in vitro*-differentiated adipocytes implanted *in vivo*. (*A* and *B*) Macroscopic aspect 2 (*A*) and 3 (*B*) weeks after implantation of the Hyaff 11 sponge seeded with adipocytes in HG-DMEM. (*Ai* and *Bi*) Images of the implanted tissue *in situ*. (*Aii*) Image of the graft after dissection. (*Bii*) Low-magnification image of the four implanted grafts. (*C* and *D*) Histological analyses of the grafts 3 weeks after implantation. Haematoxilin/eosin staining of newly formed tissues is shown. (Magnification: *Ci*, ×20; *Cii*, ×40.)

tory gene expression (24). Our results add an important conceptual mechanism by revealing a morphogenetic signaling activity of ROS. In fact, ROS, through downstream effectors and in particular through PKCβ (as revealed by the strong inhibitory effect of siRNA and by the strong synergism of high glucose with PKCβ overexpression), lead to the neoformation of adipose cells. In turn, adipocytes are known to release adipokines that regulate, among other targets, the insulin sensitivity of peripheral tissues (25). A similar role is in keeping with previous reports showing a role of ROS in embryogenesis (see, for example, the role of NOX4 in promoting the spontaneous beating of cardiac cells within embryoid bodies of mice) (26).

Finally, the present data provide additional support to the role of PKCs in detecting high-glucose conditions and sustaining the ROS-mediated signaling route. This result well agrees with a number of previous observations that on the one hand highlighted an important role for PKC in diabetes and in adipogenesis and on the other established a link between PKCs, ROS production, and cell degeneration (27). Indeed, PKC isoforms have been shown to translocate to the plasma membrane of endothelial cells upon high-glucose culture conditions (15) and to play an important role in the pathogenesis of diabetes complications. It has been recently reported that PKC-λ muscle-specific knockout mice recapitulate most of the features of the metabolic syndrome including impaired glucose tolerance or diabetes, islet β cell hyperplasia, and abdominal adiposity (28). In this case, the key dysfunction appears to be the impairment of GLUT4-mediated glucose transport across the plasma membrane of skeletal muscle, with ensuing release of anti insulinic factors and, thus, insulin resistance. In turn, insulin resistance and hyperinsulinemia can trigger abdominal obesity and adipose tissue growth in extra adipose sites such the intramuscular site. In addition to these metabolic effects, PKCs appear to be involved in detecting and decoding a variety of stress conditions, including oxidative challenges. We recently showed that PKCβ recruits the 66-kD proapoptotic isoform of Shc (p66Shc) to act as oxidoreductase within mitochondria (29) and in triggering a feed-forward cycle of ROS production eventually leading to cell death (10). The same actors may come together in a radically different context, i.e., the production of cellular signals linking hyperglicemia to the regulation of a transdifferentiation scheme of stem cells residing in insulin target tissues. How the same signaling route can trigger uncommitted stem cell differentiation or induce apoptosis remains to be elucidated. Here, we can only stress that the toxicity and the differentiation effects of H_2O_2 are optimally observed at different concentrations, i.e., 1 mM and 100 μM, respectively.

In conclusion, we demonstrate that high glucose has an adipogenic potential on stem cells derived from both the adipose tissue and skeletal muscle, and we provide some insight into the signals and molecules that underlie this process. These results may deepen our understanding of the pathogenesis of type 2 diabetes and highlight potential targets for pharmacologically addressing this disease of dramatic social impact.

Materials and Methods

Cell Cultures. ***Muscle-derived stem cells.*** Primary cultures of muscle-derived stem cells (MDSCs) were prepared from newborn rats (2–3 days) as described in ref. 5. Adipogenic conversion was observed both in the first preplating (15 min or 2 h) and in the replating of non-rapidly adherent cells. In the latter case, a small fraction of myotubes was still present, and their contraction in culture made the cell yield highly variable. For this purpose, the first pool of adherent cells was used for all experiments.

Adipose-derived stem cells. Adipose-derived stem cells (ADSCs) were extracted from human adipose tissues of five healthy female patients undergoing cosmetic surgery procedures, following guidelines from the Clinic of Plastic Surgery, University of Padova. Adipose tissues were digested with 0.075% collagenase (type 1A; Sigma–Aldrich) in Krebs–Ringer buffer (modified KRB) [125 mM NaCl, 5 mM KCl, 1 mM Na_3PO_4, 1 mM $MgSO_4$, 5.5 mM glucose, and 20 mM Hepes (pH 7.4)] for 60 min at 37°C followed by 10 min with 0.25% trypsin. Floating adipocytes were discarded, and cells from the stromal-vascular fraction were pelleted, rinsed with media, and centrifuged, and a red cell lysis step in NH_4Cl was done for 10 min at room temperature. The viable cells obtained were counted by using trypan blue exclusion assay and seeded at a density of 10×10^5 cells per square centimeter for *in vitro* expansion.

Biomaterials. Sponges made of Hyaff 11, a linear derivative of hyaluronic acid, in which the carboxylic function of the monomer glucuronic acid in the hyaluronic acid chain is totally esterified with benzyl groups, were supplied by Fidia Advanced Biopolymers. The structure of these sponges shows open interconnecting pores. Sponges were provided as cylinders. All carriers were sterilized by γ-irradiation before use.

Adipocyte Differentiation Detection. To quantitate adipocyte differentiation, Petri dish-cultured cells at days 18–25 were loaded for 10 min with 40 μM BODIPY 493/503 (4,4-difluoro-1,3,5,7,8-pentamethyl-4-bora-3a,4a-diaza-*s*-indacene; Invitrogen) and 36 μM bisbenzimide (Sigma–Aldrich), then washed with KRB. At the indicated times, oil red O (ORO) (Sigma–Aldrich) staining of the cytoplasmic droplets of neutral lipids was performed according to a modification from ref. 30. Cells cultured in the bioreactor were rinsed, fixed with 10% buffered formalin, stained with 0.3% ORO in isopropanol:water (3:2), photographed, and extracted with 4% Nonidet (Sigma–Aldrich) and isopropanol. The optical density (OD) of the solution was measured at 520 nm for quantification, using a Victor 3 spectrometer (Perkin–Elmer).

Electron Microscopy. ***SEM.*** Samples of reconstructed adipose tissues were fixed with 2.5% glutaraldehyde in 0.1 M cacodylate buffer for 1 h before being processed either with hexamethyldisilazan or at the critical point followed by gold-palladium coating. All micrographs were obtained at 30 kV on a JEOL 6360 LV SEM microscope.

TEM. Cultures were fixed in 2.5% glutaraldehyde in 0.1 M phosphate buffer pH 7.4 for 3 h, postfixed with 1% osmium tetroxide, dehydrated in a graded series of ethanol, and embedded in araldite. Semithin sections were stained with toluidine blue and used for light microscopy analysis. Ultrathin sections were stained with uranyl acetate and lead citrate and analyzed with a Philips EM400 electron microscope.

Real-Time RT-PCR and Quantitative RT-PCR. Total RNA was extracted by using a kit (RNeasy Mini; Qiagen) according to the supplier's instructions. RNA (1 μg) was treated with DNase (Ambion) and reverse-transcribed for 1 h at 37°C in a 50-μl reaction containing 1× room temperature buffer, 150 ng of random hexamers, 0.5 mmol/liter deoxynucleotide triphosphates, 20 units of RNAsin ribonuclease inhibitor, and 200 units of M-MLV RT (Promega). PCR was carried out by using a

DNA Engine Opticon 2 Continuous Fluorescence Detection System (MJ Research). All reactions were performed twice. Results were normalized by beta2microglobulin mRNA and reported as arbitrary units. The sequences of the primers are available upon request.

Analysis of PKCβ Translocation. To analyze PKCβ translocation, cells seeded onto 24-mm glass coverslips and grown in LG-DMEM for 3 days were fixed in 4% paraformaldehyde solution for 20 min at room temperature, quenched with 0.1% glycine, and permeabilized with 0.1% Triton X-100 for 20 min. After three washes with PBS, nonspecific binding sites were blocked with 2% BSA for 1 h. Immunostaining was performed with the monoclonal mouse anti-PKCβII primary antibody (diluted 1:20 in 2% BSA), followed by the visualization with the Alexa Fluor 488 anti-mouse antibody (Molecular Probes).

Measurements of ROS Production. Intracellular ROS generation was measured with 5-(and-6)-chloromethyl-2′,7′-dichlorodihydrofluorescein diacetate, acetyl ester (CM-H_2DCFDA) (Invitrogen), which is cell-permeant. After ester hydrolysis, the probe is trapped as a nonfluorescent probe, 5-(and-6)-chloromethyl-2′,7′-dichlorodihydrofluorescein. After its oxidation by ROS, 5-(and-6)-chloromethyl-2′,7′-dichlorofluorescein (CM-DCF) green emission was recorded at 520 nM.

Cells were loaded with 10 μM CM-H_2DCFDA at 37°C in modified KRB at 5.5 or 25 mM glucose. After 30 min, laser scanning confocal microscopy images were obtained. Acquisitions were made every 1 s for 500 s.

PKCβ Overexpression and Silencing. To overexpress PKCβ, the cells were transduced the day after seeding with a adenoviral vector expressing PKCβ-GFP (AdEasy/PKCβ-GFP). In the case of PKCβ overexpression in LG, we observed a decrease in cell viability 14 days after transfection, which affects the evaluation of the results. To evaluate the effect of PKCβ in LG, we compared in this experiment the efficiency of differentiation in PKCβ-expressing and control cells at an earlier time point, in which overall differentiation was lower but there was no detectable reduction in cell survival. PKCβ silencing was achieved by infecting cells the day after seeding with a commercially available lentiviral siRNA for PKCβ (Sigma–Aldrich), at a viral titol of 3.5 transduction units per milliliter. As a control, an unrelated gene (*FHIT*) was silenced, because a siRNA scrambled mixture was shown (31) and confirmed in our studies to enhance adipocyte differentiation.

Surgical Implantation of Hyaluronic Acid Sponges Seeded with Adipocytes. The protocol was approved by the Institutional Animal Care Committee of Padua University. Eight female nude rats (Charles River Laboratories), weighing 150–200 g, were subjected to the surgical procedures under halothane anesthesia and aseptic conditions. Four Hyaff 11 sponges seeded with adipocytes in HG-DMEM were implanted in the abdominal area. Throughout four small (0.3-cm) skin incisions, the sponges were inserted in a s.c. pocket above the abdominal fascia. Skin incisions were closed with one nylon 5-mm stitch. No anticoagulants were used before or after the operation, and no prophylactic antibiotic was administered. All surgical procedures were performed in the same way by a single surgeon. The animals were fed an unrestricted standard diet. After 1, 2, 3, and 4 weeks, two rats were killed by an overdose of gaseous anesthetic, and the grafts were explanted.

ACKNOWLEDGMENTS. We thank Stefano Del Prato for helpful discussion, Nicola Elvassore for the support with the bioreactor, and Marilù Fanelli for carrying out some experiments. This work was supported by Telethon Grant GGP05284, the Italian Association for Cancer Research, local funds from Ferrara University, the Italian University Ministry, the European Union Fondi Strutturali Obiettivo 2, the Programma Regionale per la Ricerca Industriale, l'Innovazione e il Trasferimento Tecnologico of the Emilia Romagna Region, the Italian Space Agency, and a National Institutes of Health Grant (1P01AG025532-01A1).

1. Timmons JA, *et al.* (2007) Myogenic gene expression signature establishes that brown and white adipocytes originate from distinct cell lineages. *Proc Natl Acad Sci USA* 104:4401–4406.
2. Fox CS, *et al.* (2007) Abdominal visceral and subcutaneous adipose tissue compartments: Association with metabolic risk factors in the Framingham Heart Study. *Circulation* 116:39–48.
3. Greco AV, *et al.* (2002) Insulin resistance in morbid obesity: Reversal with intramyocellular fat depletion. *Diabetes* 51:144–151.
4. Lexell J (1995) Human aging, muscle mass, and fiber type composition. *J Gerontol A Biol Sci Med Sci* 50(Spec No):11–16.
5. Brini M, *et al.* (1997) Subcellular analysis of Ca^{2+} homeostasis in primary cultures of skeletal muscle myotubes. *Mol Biol Cell* 8:129–143.
6. De Coppi P, *et al.* (2006) Rosiglitazone modifies the adipogenic potential of human muscle satellite cells. *Diabetologia* 49:1962–1973.
7. Grimaldi PA, Teboul L, Inadera H, Gaillard D, Amri EZ (1997) Trans-differentiation of myoblasts to adipoblasts: Triggering effects of fatty acids and thiazolidinediones. *Prostaglandins Leukotrienes Essent Fatty Acids* 57:71–75.
8. Rosen ED, Spiegelman BM (2000) Molecular regulation of adipogenesis. *Annu Rev Cell Dev Biol* 16:145–171.
9. Guillet-Deniau I, *et al.* (2004) Glucose induces *de novo* lipogenesis in rat muscle satellite cells through a sterol-regulatory-element-binding-protein-1c-dependent pathway. *J Cell Sci* 117:1937–1944.
10. Pinton P, *et al.* (2007) Protein kinase C beta and prolyl isomerase 1 regulate mitochondrial effects of the life-span determinant p66Shc. *Science* 315:659–663.
11. Schaffler A, Buchler C (2007) Concise review: Adipose tissue-derived stromal cells-basic and clinical implications for novel cell-based therapies. *Stem Cells* 25:818–827.
12. Chuang CC, Yang RS, Tsai KS, Ho FM, Liu SH (2007) Hyperglycemia enhances adipogenic induction of lipid accumulation: Involvement of extracellular signal-regulated protein kinase 1/2, phosphoinositide 3-kinase/Akt and peroxisome proliferator-activated receptor-γ (PPARγ) signaling. *Endocrinology* 148:4267–4275.
13. Farfari S, Schulz V, Corkey B, Prentki M (2000) Glucose-regulated anaplerosis and cataplerosis in pancreatic beta-cells: Possible implication of a pyruvate/citrate shuttle in insulin secretion. *Diabetes* 49:718–726.
14. Wang H, Kouri G, Wollheim C-B (2005) ER stress and SREBP-1 activation are implicated in beta-cell glucolipotoxicity. *J Cell Sci* 118:3905–3915.
15. Gallo A, *et al.* (2005) Metformin prevents glucose-induced protein kinase C-beta2 activation in human umbilical vein endothelial cells through an antioxidant mechanism. *Diabetes* 54:1123–1131.
16. Vertino AM, *et al.* (2005) Wnt10b deficiency promotes coexpression of myogenic and adipogenic programs in myoblasts. *Mol Biol Cell* 16:2039–2048.
17. Renault V, *et al.* (2000) Skeletal muscle regeneration and the mitotic clock. *Exp Gerontol* 35:711–719.
18. Conboy IM, Conboy MJ, Smythe GM, Rando TA (2003) Notch-mediated restoration of regenerative potential to aged muscle. *Science* 302:1575–1577.
19. Goodpaster BH, He J, Watkins S, Kelley DE (2001) Skeletal muscle lipid content and insulin resistance: Evidence for a paradox in endurance-trained athletes. *J Clin Endocrinol Metab* 86:5755–5761.
20. Taylor-Jones JM, *et al.* (2002) Activation of an adipogenic program in adult myoblasts with age. *Mech Ageing Dev* 123:649–661.
21. Brownlee M (2001) Biochemistry and molecular cell biology of diabetic complications. *Nature* 414:813–820.
22. Turrens JF (2003) Mitochondrial formation of reactive oxygen species. *J Physiol* 552:335–344.
23. Rattan SI (2006) Theories of biological aging: Genes, proteins, and free radicals. *Free Radic Res* 40:1230–1238.
24. Zmijewski JW, Zhao X, Xu Z, Abraham E (2007) Exposure to hydrogen peroxide diminishes NF-κB activation, IκB-α degradation, and proteasome activity in neutrophils. *Am J Physiol* 293:C255–C266.
25. Yang Q, *et al.* (2005) Serum retinol binding protein 4 contributes to insulin resistance in obesity and type 2 diabetes. *Nature* 436:356–362.
26. Li J, *et al.* (2006) The NADPH oxidase NOX4 drives cardiac differentiation: Role in regulating cardiac transcription factors and MAP kinase activation. *Mol Biol Cell* 17:3978–3988.
27. Avignon A, Sultan A (2006) PKC-B inhibition: A new therapeutic approach for diabetic complications? *Diabetes Metab* 32:205–213.
28. Farese RV, *et al.* (2007) Muscle-specific knockout of PKC-lambda impairs glucose transport and induces metabolic and diabetic syndromes. *J Clin Invest* 117:2289–2301.
29. Giorgio M, *et al.* (2005) Electron transfer between cytochrome c and p66Shc generates reactive oxygen species that trigger mitochondrial apoptosis. *Cell* 122:221–233.
30. Ramirez-Zacarias JL, Castro-Munozledo F, Kuri-Harcuch W (1992) Quantitation of adipose conversion and triglycerides by staining intracytoplasmic lipids with oil red O. *Histochemistry* 97:493–497.
31. Xu Y, Mirmalek-Sani SH, Lin F, Zhang J, Oreffo RO (2007) Adipocyte differentiation induced using nonspecific siRNA controls in cultured human mesenchymal stem cells. *RNA* 13:1179–1183.